Structural Engineering and Mechanics, Vol. 29, No. 2 (2008) 135-154
DOI: http://dx.doi.org/10.12989/sem.2008.29.2.135

A MOM-based algorithm for moving force identification: Part I – Theory and numerical simulation

Ling Yu

Key Lab of Disaster Forecast and Control in Engineering, Ministry of Education of the People's Republic of China (Jinan University), Guangzhou 510632, P. R. China
Department of Civil and Structural Engineering, The Hong Kong Polytechnic University, Hong Kong, P. R. China

Tommy H.T. Chan†

School of Urban Development, Faculty of Built Environment & Engineering, Queensland University of Technology, GPO Box 2434, Queensland 4001, Australia
Department of Civil and Structural Engineering, The Hong Kong Polytechnic University, Hong Kong, P. R. China

Jun-hua Zhu

Key Lab of Disaster Forecast and Control in Engineering, Ministry of Education of the People's Republic of China (Jinan University), Guangzhou 510632, P. R. China
Changjiang River Scientific Research Institute, Wuhan 430010, P. R. China

(Received August 30, 2006, Accepted August 7, 2007)

Abstract. The moving vehicle loads on a bridge deck is one of the most important live loads of bridges. They should be understood, monitored and controlled before the bridge design as well as when the bridge is open for traffic. A MOM-based algorithm (MOMA) is proposed for identifying the time-varying moving vehicle loads from the responses of bridge deck in this paper. It aims at an acceptable solution to the ill-conditioning problem that often exists in the inverse problem of moving force identification. The moving vehicle loads are described as a combination of whole basis functions, such as orthogonal Legendre polynomials or Fourier series, and further estimated by solving the new system equations developed with the basis functions. A number of responses have been combined, some numerical simulations on single axle, two axle and multiple-axle loads, being either constant or time-varying, have been carried out and compared with the existing time domain method (TDM) in this paper. The illustrated results show that the MOMA has higher identification accuracy and robust noise immunity as well as producing an acceptable solution to ill-conditioning cases to some extent when it is used to identify the moving force from bridge responses.

Keywords: moving force identification; method of moments (MOM); bridge-vehicle interaction; time domain method; legendre polynomials; fourier series.

---

† Ph.D., Corresponding author, E-mail: tommy.chan@qut.edu.au

1. Introduction

The study of moving vehicle loads on bridge deck is an important issue from the aspects of design, diagnosis and maintenance of bridges, as they contribute to the live load component in a bridge design code (Ting and Yener 1983). Direct measurements of the forces using instrumented vehicles are expensive and are subjected to bias (Cantineni 1992, Heywood 1994). Systems have been developed for so called 'weigh-in-motion' of vehicles (Peters 1984, 1986), but they all measure only the equivalent static axle loads. It has been observed that the induced dynamic deflection and stresses can be a significantly higher than those observed in the static case as a structure is subjected to moving loads, for example, a dynamic increment of 125% was obtained on a small composite bridge (Chan and O'Conner 1990).

In the last decade, a few indirect identification methods were successively proposed and incorporated into a moving force identification system (MFIS) (Yu 2002). Numerical simulations, illustrative examples and comparative studies show that each method involved in the MFIS could effectively identify moving forces with acceptable accuracy and both time domain method (TDM) and frequency time domain method (FTDM) were found better than others (Chan *et al.* 2001). However, there still exist some limitations if these methods could actually be operated in practice. For example, the identification results were sensitive to noise as they are the natural output of an ill-conditioned inverse problem. The TDM and FTDM have higher identification accuracy but they are time consuming. The CPU executive time for both the Interpretation Method I (IMI) and II (IMII) are shorter, but their identification accuracy is less than that from both the TDM and FTDM (Chan *et al.* 2001).

In fact, there is a convolution integral relationship between the bridge responses and the moving loads on a bridge in time domain in terms of structural dynamics. The integral equations are often discretized with the method of moments (MOM) (Harriington 1968) which is one of the most widespread and generally accepted techniques for electromagnetic problems (Jorgensen *et al.* 2004, Pawlak 1992, Chew *et al.* 2001, Qjidaa and Radouane 1999, Liao and Pawlak 1996), as it requires less unknowns than techniques based on differential equations (Jorgensen *et al.* 2004) and it is robustness for noise and digitizing (Pawlak 1992). However, at the same time it necessitates the solution of a matrix system with a dense and often ill-conditioned matrix (Chew *et al.* 2001). This requires a set of basis functions that does not lead to an ill-conditioned matrix. The selection of basis functions is a crucial point when solving the integral equation by the MOM. Various moments, including geometric, complex, Legendre, Zernike, Pseudo-Zernike, Fouries-Mellin, radial, and orthogonal moments may be used (Pawlak 1992, Qjidaa and Radouane 1999), in which Legendre or Zernike moments are better than the others, and the Fourier moments are not time-consuming (Qjidaa and Radouane 1999). Here, we will use Legendre and Fourier moments because of the efficient algorithms for their computation (Liao and Pawlak 1996).

In this paper, based on the MOM and the theory of moving force identification, a MOM-based algorithm (MOMA) is proposed for identifying the dynamic axle loads with the aim to overcome the limitations induced from the ill-conditioned problem. The moving vehicles loads were described as a combination of whole basis functions, and further were estimated by solving the new system equations developed with the basis functions. Two solutions to the over-determined set of system equations, the singular value decomposition (SVD) and the Tikhonov regularization method, are introduced and some simulations have been conducted. Compared with the existing time domain method (TDM), the illustrated results show that the MOMA has higher identification accuracy, less noise sensitive and an acceptable solution to the ill-conditioned problem to some extent when the basis functions number were adopted properly. If the Tikhonov regularization method was used, the identification results of both the TDM and MOMA would be improved, especially for the TDM.

2. Background of theory

2.1 Motion equation of bridge-vehicle system

A bridge superstructure is modeled with a simply supported beam as shown in Fig. 1. The effects of shear deformation and rotary inertia are not taken into account (Bernoulli-Euler beam). If the force $f(t)$ moves from left to right at a speed c, then an equation of motion in terms of modal coordinate $q_n(t)$ can be expressed as

$$\ddot{q}_n(t) + 2\xi_n\omega_n\dot{q}_n(t) + \omega_n^2 q_n(t) = \frac{2}{\rho L}p_n(t), \quad (n = 1, 2, \ldots, \infty) \tag{1}$$

Where

$$\omega_n = \frac{n^2\pi^2}{L^2}\sqrt{\frac{EI}{\rho}}, \quad \xi_n = \frac{C}{2\rho\omega_n}, \quad p_n(t) = f(t)\cdot\sin\frac{n\pi ct}{L} \tag{2}$$

They are the nth modal frequency, the modal damping ratio and the modal force, respectively. ρ and L are the constant mass per unit length and the span length of bridge respectively. The moving force identification is an inverse problem in structural dynamics, in which the unknown time-varying force $f(t)$ is identified from measured displacements, accelerations or bending moments of real structures.

2.2 Method of Moments (MOM) and basis functions

2.2.1 Method of Moments (MOM)

The MOM is a general procedure for solving linear equations of the type $L \bullet f = R$, where L is an integro-differential operator, R is a known vector function, and f is an unknown vector function. Let f be expanded in a series of $f_1, f_2, f_3, \ldots$ in the domain of L, as

$$f = \sum_n \alpha_n f_n \tag{3}$$

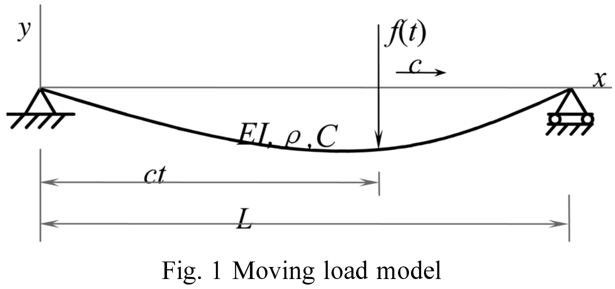

Fig. 1 Moving load model

where, the α_n are the constants, the f_n are the *expansion functions* or *basis functions*. For exact solutions, Eq. (3) is usually an infinite summation and the f_n form a complete set of basis functions. For approximate solutions, Eq. (3) is usually a finite summation. Substituting Eq. (3) into $L \bullet f = R$, and using the linearity of L, we have

$$\sum_n \alpha_n L f_n = R \tag{4}$$

It is assumed that a suitable inner product $<f, R>$ has been determined for the problem. Now define a set of *weighting functions*, or *testing functions*, $w_1, w_2, w_3, \ldots$ in the range of L, and take the inner product of Eq. (4) with each w_m. The result is

$$\sum_n \alpha_n <w_m, Lf_n> = <w_m, R> \tag{5}$$

$m = 1, 2, 3, \ldots$. Discretizing the equation $L \bullet f = R$ via the above procedure of the MOM yields the matrix equation $[l_{mn}]\ \{\alpha_n\} = \{R\}$. If the matrix $[l]$ is nonsingular, its inverse $[l^{-1}]$ exists. The a_n are then given by $\{\alpha_n\} = [l_{mn}^{-1}]\{R_m\}$ and the solution for f is given by Eq. (3). The solution may be exact or approximate, depending upon the choice of the basis functions f_n and weighting functions w_n. The particular choice $w_n = f_n$ is known as Galerkin's method (Harriington 1968).

2.2.2 Basis functions

The selection of basis functions is a crucial point when solving the integral equation by the MOM. Here, the orthogonal Legendre polynomials and Fourier series are selected as the basis functions because of the efficient algorithms for their computation (Liao and Pawlak 1996) as well as their better features than others (Pawlak 1992, Qjidaa and Radouane 1999).

2.2.2.1 Legendre polynomials

For each order of n, the Legendre polynomials can be defined by either the series

$$P_n(t) = \sum_{k=0}^{[n/2]} \frac{(-1)^k (2n-2k)!}{2^n k!(n-k)!(n-2k)!} t^{n-2k} \tag{6}$$

$$[n/2] = \begin{cases} n/2 & n = even \\ (n-1)/2 & n = odd \end{cases}$$

or the recurrence formula (Poularikas 1999)

$$(n+1)P_{n+1}(t) = (2n+1)tP_n(t) - nP_{n-1}(t-1), \quad (n = 1, 2, \ldots,\ t \in [-1, 1]) \tag{7}$$

where $P_0(t) = 0$ and $P_1(t) = t$. The first few Legendre polynomials are listed as

$$P_0(t) = 1$$

$$P_1(t) = t$$

$$P_2(t) = 1/2(3t^2 - 1)$$

$$P_3(t) = 1/2(5t^3 - 3t)$$

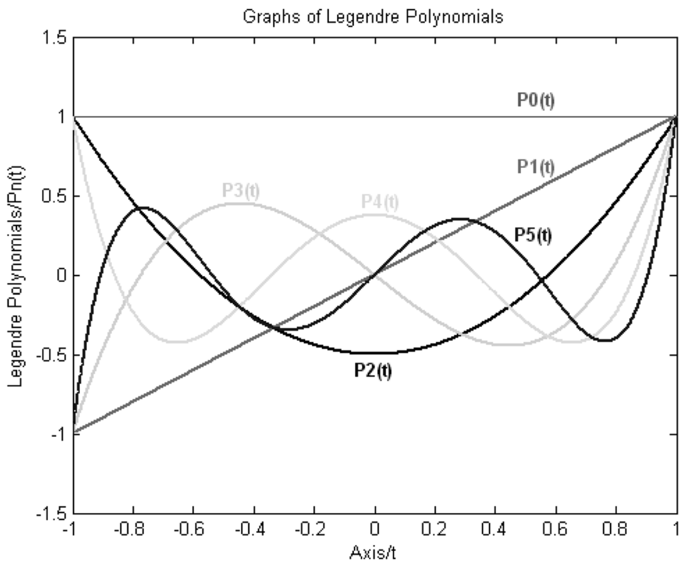

Fig. 2 Graphs of Legendre polynomials $P_n(t)$ (n = 0, 1, 2, 3, 4, 5)

$$P_4(t) = 1/8(35t^4 - 30t^2 + 3)$$
$$P_5(t) = 1/8(63t^5 - 70t^3 + 15t)$$

The graphs of Legendre polynomials $P_n(t)$, $n = 0, 1, 2, 3, 4, 5$, are sketched in Fig. 2 over the interval [−1, 1].

Their orthogonality are expressed as follows

$$\int_{-1}^{1} P_n(t) \cdot P_m(t) \cdot dt = \begin{cases} \dfrac{2}{2n+1} & m = n \\ 0 & m \neq n \end{cases} \tag{8}$$

If a function $f(t)$ is defined in the interval [0, s], it is necessary in the application to expand the function in a series in the application to expand the function in a series of orthogonal polynomials in this interval. Clearly transforming the interval [0, s] into the interval [−1, 1] in the time domain, therefore, Eq. (7) can be rewritten as

$$P_0(t) = 1,\ P_1(t) = 2t/s - 1,\ \ldots$$
$$(n + 1) \cdot P_{n+1}(t) = (2n + 1) \cdot (2t/s - 1) \cdot P_n(t) - n \cdot P_{n-1}(t) \qquad (n \geq 1,\ t \in [0, s]) \tag{9}$$

2.2.2.2 Fourier series

Assuming the time-varying load function $f(t)$ satisfies the Dirichlet conditions, the Fourier series corresponding to the function $f(t)$ is

$$f(t) = \frac{a_0}{2} + \sum_{k=1}^{\infty}\left(a_k\cos\frac{k\pi ct}{L} + b_k\sin\frac{k\pi ct}{L}\right) \qquad t \in \left[-\frac{L}{c}, \frac{L}{c}\right] \tag{10}$$

Setting the function $f(t)$ to be an even or odd function and considering the shape of function $f(t)$ in the time interval [0, L/c] only, Eq. (10) can be simplified as

$$f(t) = \frac{a_0}{2} + \sum_{k=1}^{\infty} a_k \cos\frac{k\pi ct}{L} \quad \text{(while } f(t) \text{ is even function)} \tag{11a}$$

$$f(t) = \sum_{k=1}^{\infty} b_k \sin\frac{k\pi ct}{L} \quad \text{(while } f(t) \text{ is odd function)} \tag{11b}$$

2.3 Moving force identification based on Method of Moments (MOM)

The method of moments is based on the radical idea that the functional equation is rewritten in discrete terms. Assuming $f(t)$ can be expressed as follows in terms of a series of basis function $\psi_0(t)$, $\psi_1(t)$, $\psi_2(t)$, …, $\psi_n(t)$.

$$f(t) = \sum_k \alpha_k \psi_k(t) \tag{12}$$

Arranging Eq. (12) into a matrix form

$$\{f\} = [\Psi] \cdot \{\alpha\} \tag{13}$$

Where $\psi_k(t) = P_k(t)$ or $\psi_k(t) = \sin(k\pi ct/L)$, representing the basis functions, are the Legendre polynomials or Fourier series respectively in this paper.

2.3.1 Identification from bending moment responses

Eq. (1) can be solved in time domain by the convolution integral and the dynamic deflection $v(x, t)$ of the beam at point x and time t can be obtained as (Chan *et al.* 2001)

$$v(x,t) = \sum_{n=1}^{\infty} \frac{2}{\rho L \omega'} \sin\frac{n\pi x}{L} \int_0^t e^{-\xi_n \omega_n (t-\tau)} \sin\omega_n'(t-\tau) \sin\frac{n\pi c\tau}{L} f(\tau) d\tau \tag{14}$$

Where $\omega_n' = \omega_n\sqrt{1-\xi_n^2}$, therefore the bending moment of the beam at point x and time t is

$$m(x,t) = -EI\frac{\partial^2 v(x,t)}{\partial x^2}$$

$$= \sum_{n=1}^{\infty} \frac{2EI\pi^2}{\rho L^3} \frac{n^2}{\omega_n'} \sin\frac{n\pi x}{L} \int_0^t e^{-\xi_n \omega_n (t-\tau)} \sin\omega_n'(t-\tau) \sin\frac{n\pi c\tau}{L} f(\tau) d\tau \tag{15}$$

Let the test function $\omega_j = \delta(t - t_j)$, after substituting Eq. (12) into Eq. (15), multiplying by ω_j, integrating the resultant equation with respect to t between 0 and infinite, and using the properties of the test function ω_j, the Eq. (15) can be expressed as

$$m(x,t_j) = \sum_{k=0}^{m} \alpha_k \cdot l_{jk} \quad (j = 0, 1, \ldots, N) \tag{16}$$

$$l_{jk} = \sum_{n=1}^{\infty} \frac{2EI\pi^2}{\rho L^3} \frac{n^2}{\omega_n'} \sin\frac{n\pi x}{L} \int_0^{t_k} e^{-\xi_n\omega_n(t_j-\tau)} \sin\omega_n'(t_j-\tau) \sin\frac{n\pi c\tau}{L} \psi_k(\tau) d\tau \tag{17}$$

Where, the superscript m is the basis functions number, $t_j = j\Delta t$, Δt is the sampling interval and N is the number of sample points for the measured bending moment responses.

Eqs. (16) and (17) can be rewritten in discrete terms and rearranged into a set of equations

$$\underset{(N-1)\times 1}{M} = \underset{(N-1)\times(m+1)}{L} \cdot \underset{(m+1)\times 1}{\alpha} \tag{18}$$

$$\underset{(N-1)\times(m+1)}{L} = \underset{(N-1)\times(N_B-1)}{B} \cdot \underset{(N_B-1)\times(m+1)}{\Psi} \tag{19}$$

Where, $\Psi = \begin{bmatrix} \psi_0(1) & \psi_1(1) & \dots & \psi_m(1) \\ \psi_0(2) & \psi_1(2) & \dots & \psi_m(2) \\ \vdots & \vdots & \ddots & \vdots \\ \psi_0(N_B-1) & \psi_1(N_B-1) & \dots & \psi_m(N_B-1) \end{bmatrix}$, $M = \begin{Bmatrix} m(2) \\ m(3) \\ \vdots \\ m(N) \end{Bmatrix}$ and $\alpha = \begin{Bmatrix} \alpha_0 \\ \alpha_1 \\ \vdots \\ \alpha_m \end{Bmatrix}$

are the matrix of basis functions, the time-series vector of the measured bending moment responses and the coefficient vector respectively. B refers to the reference (Law *et al.* 1997).

If $N - 1 = m + 1$, the coefficient α can be obtained directly by solving Eq. (18). If $N - 1 > m + 1$ or $N - 1 < m + 1$, the least-squares method can be used to find the coefficient α, and then substituting α into Eq. (13), the time history of the moving loads can be obtained finally.

2.3.2 Identification from accelerations

The accelera $\ddot{v}(x,t)$ at point x and time t is

$$\ddot{v}(x,t) = \sum_{n=1}^{\infty} \frac{2}{\rho L} \sin\frac{n\pi x}{L} \left[f(t)\sin\frac{n\pi ct}{L} + \int_0^t \ddot{h}_t(t-\tau) f(\tau) \sin\frac{n\pi c\tau}{L} d\tau \right] \tag{20}$$

Where $$\ddot{h}_t(t) = \frac{1}{\omega_n'} e^{-\xi_n\omega_n t} \{ [(\xi_n\omega_n)^2 - \omega_n'^2] \sin\omega_n' t + [-2\xi_n\omega_n\omega_n'] \cos\omega_n' t \}$$

After substituting Eq. (12) into Eq. (20), multiplying by ω_j, integrating the resultant equation with respect to t between 0 and infinite, and using the properties of the test function ω_j, the acceleration response of the beam can be expressed as in discrete terms

$$\underset{N\times 1}{\ddot{V}} = \underset{N\times(m+1)}{H} \cdot \underset{(m+1)\times 1}{\alpha} \tag{21}$$

Where $\underset{N\times(m+1)}{H} = \underset{N\times(N_B-1)}{A} \cdot \underset{(N_B-1)\times(m+1)}{\Psi}$, A refers to the reference (Law *et al.* 1997).

The coefficient α can be calculated by solving the Eq. (21), and then substituting α into Eq. (13), the force vector $\{f\}$ can be found.

2.3.3 Identification from combination of bending moments and accelerations

If the bending moments and the acceleration responses are measured at the same time, both of them can be used together to identify the moving force. The vectors M in Eq. (18) and $\ddot{V}$ in Eq. (21) should be scaled to have dimensionless units; then the two equations can be combined, to give

$$\begin{bmatrix} L/\|M\| \\ H/\|\ddot{V}\| \end{bmatrix} \cdot \alpha = \begin{Bmatrix} M/\|M\| \\ \ddot{V}/\|\ddot{V}\| \end{Bmatrix} \tag{22}$$

Where $\|\bullet\|$ is the norm of a matrix.

The above procedure is derived for the identification of a single force. They can be modified for the identification of multi-forces in terms of the linear superposition principle.

2.4 Solutions

As mentioned above, it is easy to see that both the MOMA and the TDM will usually result in a system of equation with the form

$$Ax = b \tag{23}$$

Where, x is the unknown load vector, b is the time series vector of the measured bending moment or acceleration response. The system matrix A is associated with the bridge-vehicle system. In principle, Eq. (23) will have a solution given by the least-squares method as

$$x = A^{+}b \tag{24}$$

Assuming the size of matrix A belongs to $k \times n$, if $k > n$ then the system $Ax = b$ is an over-determined system of equation, $A^{+} = (A^{T}A)^{-1}A^{T}$, if $k < n$, Eq. (23) is an under-determined equation, $A^{+} = A^{T}(AA^{T})^{-1}$.

2.4.1 Singular Value Decomposition (SVD) solution

As matrix A is usually close to rank deficient, A^{+} is best calculated from the singular value decomposition (SVD) of A (Lindfield and Penny 1995). The SVD technique, applied to structural dynamics problems in the last fifteen years, is one of the most important tools in numerical analysis. If matrix A is real, the SVD of A is USV^{T}, its inverse can easily be calculated from $A^{+} = VS^{-1}U^{T}$. For simplicity, assuming that A has no exact zero singular values, it can be shown that the least squares solution vector x is given by

$$x = \sum_{i=1}^{\min(k,n)} \frac{u_i^T b_i}{\sigma_i} v_i \tag{25}$$

The solution vector x here is called SVD solution. Eq. (25) clearly illustrates the difficulties associated with standard matrix solutions of Eq. (23). If the numerator does not decay as fast as the singular value σ_i of the denominator, the solution is dominated by terms containing the smallest σ_i. Consequently, the solution x may have many sign changes and thus appears to be random. When A is rank deficient, only the $r(r \le \min(k, n))$ non-zero singular values of the matrix are taken into account so that S is a $r \times r$ matrix where r is the rank of A. to make the multiplication of Eq. (25) conformable, the first r columns of V and the first r columns of U in Eq. (25) are used.

2.4.2 Regularization solution

For the moving force identification problem, since the solution to Eq. (23) is ill-conditioned, the regularization method developed by Tikhonov and Arsenin (Tikhonov and Arsenin 1977) can be used to provide bounds to the solution. The Tikhonov regularization method is based on the radical idea that minimizes the deviations of Ax from b in Eq. (23) for a stable solution by means of an auxiliary non-negative parameter. This is equivalent to imposing certain constraints in the form of added penalty terms with adjustable weighting (regularization) parameters to the solution. The Tikhonov function can be defined as

$$J(x, \lambda) = \|Ax - b\|^2 + \lambda\|x\|^2 \tag{26}$$

Where λ is a non-negative regularization parameter, the solution of Eq. (26) is obtained in the Tikhonov regularization with the damped least-squares method as (Santantamarina and Fratta 1998)

$$x = (A^T A + \lambda I)^{-1} A^T b \tag{27}$$

Where I is an identity matrix and the singular value decomposition (SVD) is used in the pseudo inverse calculation. Applying the Tikhonov regularization, the main difficulty is how to effectively find the optimal regularization parameters λ (Law *et al.* 2001)). Here, the generalized cross-validation (GCV) method is used to determine the optimal parameter λ and the S-curve method is used to plot the error against the different parameter λ (Busby and Trujillo 1997). If the true force f_{true} were known, the true force is compared with the identified values $f_{identified}$, and the relative quadratic percentage error (RQPE) between the time histories of true force f_{true} and identified force $f_{identified}$ is defined as

$$RQPE = \frac{\|f_{identified} - f_{true}\|}{\|f_{true}\|} \times 100\% \tag{28}$$

As an example, a typical S-curve is shown in Fig. 3. It is clearly noted from Fig. 3 that the optimal regularization parameter λ corresponds to the minimum RQPE value.

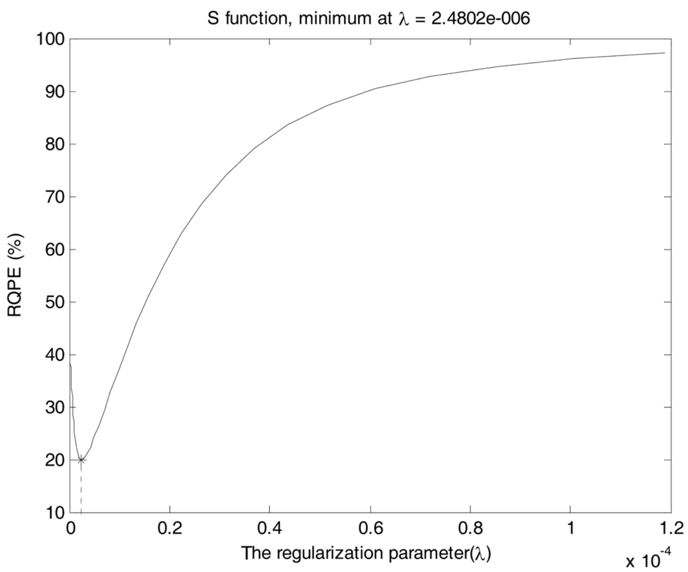

Fig. 3 Typical S-curve under 10% noise

3. Numerical simulation

3.1 Bridge-vehicle and simulation parameters considered

In order to check the correctness and effectiveness of the proposed method, the following moving force identification cases are simulated and illustrated.

(a) Single vehicle load

$$f(t) = 40\ 000 \times [1 + 0.1 \sin(10\pi t) + 0.05 \sin(40\pi t)]\ N$$

(b) Two-axle vehicle loads

(i) Constant loads

$$f_1(t) = 58\ 800 \text{ N}$$
$$f_2(t) = 137\ 200 \text{ N}$$
$$s = 8 \text{ m}$$

(ii) Time-varying loads

$$f_1(t) = 58\ 800 \times [1 + 0.1 \sin(10\pi t) + 0.05 \sin(40\pi t)] \text{ N}$$
$$f_2(t) = 137\ 200 \times [1 - 0.1 \sin(10\pi t) + 0.05 \sin(50\pi t)] \text{ N}$$
$$l_s = 8 \text{ m}$$

(c) Multi-axle vehicle loads

(i) Constant loads

$$f_1(t) = 58\ 800 \text{ N}$$
$$f_2(t) = 137\ 200 \text{ N}$$
$$f_3(t) = 150\ 000 \text{ N}$$
$$l_{s1} = 3 \text{ m}, \quad l_{s2} = 2.5 \text{ m}.$$

(ii) Time-varying loads

$$f_1(t) = 58\ 800 \times [1 + 0.1 \sin(10\pi t) + 0.05 \sin(40\pi t)] \text{ N}$$
$$f_2(t) = 137\ 200 \times [1 - 0.1 \sin(10\pi t) + 0.05 \sin(50\pi t)] \text{ N}$$
$$f_3(t) = 150\ 000 \times [1 + 0.1 \sin(10\pi t) + 0.05 \sin(40\pi t)] \text{ N}$$
$$l_{s1} = 3 \text{ m}, l_{s2} = 2.5 \text{ m}.$$

The parameters of the beam bridge are as follows: $EI = 1.27914 \times 10^{11}$ N·m^2, $\rho = 12\ 000$ kg/m, $L = 40$ m, $f_1 = 3.2$ Hz, $f_2 = 12.8$ Hz, $f_3 = 28.8$ Hz. The moving speed $c = 40$ m/s. the analysis frequency bandwidth is from 0 Hz to 40 Hz and therefore the first three modes of the beam are included in the calculation. The sampling frequency f_s is 200Hz (Yu 2002, Chan *et al.* 2001, Law *et al.* 1997).

Random noise is added to the calculated responses to simulate the polluted measurements as

$$R_{measured} = R_{calculated} \cdot (1 + Ep \cdot N_{oise}) \tag{29}$$

Where Ep represents specified error level ranging from 0.0 to 1.0; N_{oise} is a standard normal distribution vector with zero mean value and unit standard deviation.

3.2 Study cases

3.2.1 Single vehicle load

Bending moment and/or acceleration responses at 1/2 span and/or 1/4 span are used to identify the single moving load. Nine sensor arrangement cases are studied, and Table 1 and Table 2 show the comparison on the relatively quadratic percentage error (RQPE) values between the true and the identified loads respectively by the SVD and the regularization solution. In the table, the letters '*m*' and '*a*' represent the bending moment and acceleration responses respectively, which are used to identify the single moving load. Fractions 1/4 and 1/2 represent the measurement locations at quarter and middle spans respectively. Underlined RQPE values result from Fourier series basis functions, the values in parentheses from Legendre polynomial basis functions. There are same meanings in the following tables if no further stated. From Tables 1 and 2, it can be found that:

(1) Whether under 1% or under 5% noise levels as listed in Table 1, the MOMA results are

Table 1 Comparison on RQPE of single load identified via SVD

Sensor location	1% Noise			5% Noise		
	TDM	MOMA		TDM	MOMA	
1/4m	43.8	<u>1.33</u>	(3.77)	*	<u>6.66</u>	(18.9)
1/2m	*	<u>4.02</u>	(6.15)	*	<u>20.1</u>	(30.7)
1/4m&1/2m	21.8	<u>1.08</u>	(2.48)	*	<u>5.38</u>	(12.3)
1/4a	1.03	<u>0.32</u>	(0.34)	5.17	<u>1.61</u>	(1.72)
1/2a	1.21	<u>0.18</u>	(0.39)	6.03	<u>0.92</u>	(1.96)
1/4a&1/2a	0.27	<u>0.12</u>	(0.17)	1.34	<u>0.61</u>	(0.84)
1/2m&1/2a	0.87	<u>0.23</u>	(0.25)	4.37	<u>1.15</u>	(1.24)
1/4m&1/4a	0.78	<u>0.14</u>	(0.16)	3.89	<u>0.69</u>	(0.83)
1/2m&1/4a	0.85	<u>0.20</u>	(0.21)	4.26	<u>0.97</u>	(1.08)

Note: * indicates the RQPE exceeds 100%, 1/4 and 1/2 represent the measurement location at a quarter, middle span respectively. Underlined values are for Fourier basis functions, and values in parentheses for Legendre basis functions.

Table 2 Comparison on RQPE of single load identified via regularization

Sensor location	1% Noise			5% Noise		
	TDM	MOMA		TDM	MOMA	
1/4m	11.6	<u>1.33</u>	(3.46)	21.6	<u>6.66</u>	(14.1)
1/2m	12.7	<u>4.02</u>	(5.08)	22.9	<u>15.2</u>	(18.4)
1/4m&1/2m	9.88	<u>1.08</u>	(1.86)	18.7	<u>5.38</u>	(9.23)
1/4a	1.03	<u>0.32</u>	(0.34)	5.17	<u>1.61</u>	(1.59)
1/2a	1.21	<u>0.18</u>	(0.27)	6.02	<u>0.91</u>	(1.73)
1/4a&1/2a	0.27	<u>0.12</u>	(0.16)	1.34	<u>0.61</u>	(0.72)
1/2m&1/2a	0.87	<u>0.22</u>	(0.25)	3.74	<u>1.12</u>	(1.20)
1/4m&1/4a	0.78	<u>0.14</u>	(0.15)	3.84	<u>0.69</u>	(0.66)
1/2m&1/4a	0.85	<u>0.20</u>	(0.21)	4.15	<u>0.97</u>	(1.02)

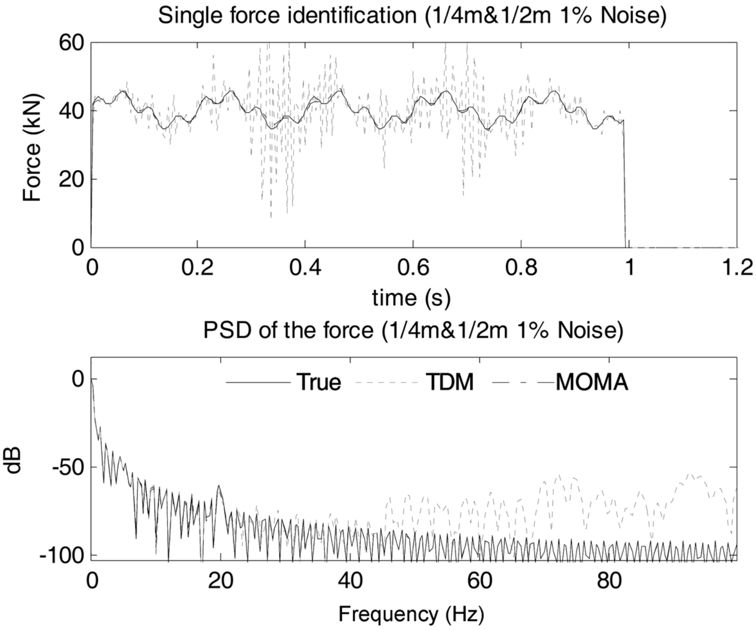

Fig. 4 Single load identified from bending moment responses (1/4m&1/2m, Fourier basis function, SVD)

clearly better than the TDM results when the SVD solution is adopted. The MOMA has clearly higher identification accuracy and is less sensitive to noise than the TDM for all cases, whether using Fourier series or using Legendre polynomial basis functions. For the MOMA, if the Fourier series basis functions are adopted, the identified results are better than those using the Legendre polynomial basis functions. However, the RQPE values by both the TDM and MOMA method are increasing as the noise level increases. In addition, when the SVD is adopted under the 1% noise, Fig. 4 shows the time histories and their power spectral density (PSD) of the moving true and identified loads when the single moving time-varying load is identified from two bending moment responses at 1/4m&1/2m. It can be seen that the MOMA is a good agreement with the true load, but the TDM does not agree with the true load because it clearly includes the significant higher frequency components after the 40 Hz.

(2) For case comparison, Table 1 also shows that the RQPE values can be dramatically reduced if the bending moment responses are partly or completely replaced with the acceleration responses at the same sensor locations, especially for the TDM. Obviously, two responses are used to identify the single moving load, the corresponding results are better than those by only using one response for the TDM. For the MOMA, there are same conclusions when the Legendre basis functions are adopted. However, if the Fourier basis functions are adopted, there is a different conclusion. In fact, the RQPE values from one acceleration response are close to the results by using responses from two combination sensor locations, i.e., one bending moment and one acceleration response. In addition, when the SVD is adopted under the 5% noise, Fig. 5 also shows the time histories and their PSD of the moving true and identified loads when the single moving time-varying load is identified from two acceleration responses at 1/4a&1/2a. It can be seen that both the TDM and the MOMA are in good agreement with the true load, whether from the time histories or from their PSD curves.

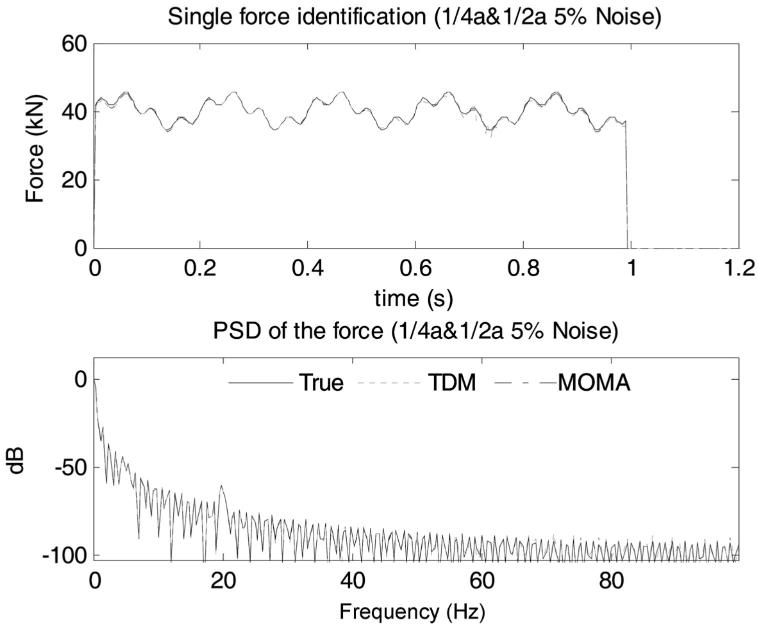

Fig. 5 Single load identified from two acceleration responses (1/4a&1/2a, Fourier basis function, SVD)

(3) If the regularization solution is adopted, it can be seen from Table 2 that the TDM results are greatly improved when compared with the RQPE values by SVD solution in Table 1, especially when only the bending moment responses are used to identify the single moving load. Even so, the TDM results are still much worse than the MOMA results. For the MOMA, the identified results can also be slightly improved when the Legendre basis functions are adopted, particularly under the higher 5% noise level. When the Fourier basis functions are adopted for the MOMA, or when only the acceleration responses or the combination of bending moment and acceleration responses are used for the TDM, there are almost no difference between the regularization results in Table 2 and the SVD results in Table 1.

(4) From the RQPE values in Tables 1 and 2, it can be found that the MOMA identification results, adopting either Fourier basis function or Legendre basis function, are close to each other, especially when only the acceleration responses or the combination of bending moment and acceleration responses are used to identify the moving loads. In addition, the MOMA has higher computation efficiency when Fourier basis function is adopted. Therefore, the Fourier basis functions are only adopted for the MOMA in the following studies.

3.2.2 Two axle vehicle loads (Constant and Time-varying Loads)

In order to evaluate the correctness of MOMA for the identification of two axle vehicle loads, the MOMA are also used to identify both the two axle constant and time-varying loads from bending moment and/or acceleration responses at 1/4, 1/2, and 3/4 spans in twelve combination cases. Table 3 shows the comparison on the RQPE values of two axle constant loads identified by both the TDM and MOMA under the 5% noise level as well as including the effect of two different solutions, i.e. the SVD and regularization solutions. Selecting four out of twelve combination cases, Table 4 gives the comparison on the RQPE values of two axle time-varying loads identified by TDM and MOMA

Table 3 Comparison on RQPE of two axle constant loads under 5% noise

Sensor location	TDM				MOMA			
	Axle 1		Axle 2		Axle 1		Axle 2	
1/4m&1/2m	*	36.5	*	28.5	1.06	0.76	0.25	0.05
1/4m&1/2m&3/4m	*	34.4	*	27.6	0.79	0.39	0.37	0.04
1/4a&1/2a	55.8	14.1	25.8	10.9	0.18	0.18	0.24	0.24
1/4a&1/2a&3/4a	2.58	2.58	1.40	1.40	0.10	0.10	0.21	0.21
1/2m&1/2a	*	35.0	*	24.6	0.26	0.26	0.15	0.15
1/4m&1/2m&1/2a	*	25.2	*	23.2	0.13	0.13	0.11	0.11
1/4m&1/2m&1/4a&1/2a	55.0	16.6	25.9	10.8	0.04	0.04	0.18	0.18
1/4m&1/4a	*	28.2	*	23.5	0.17	0.17	0.20	0.20
1/4m&1/4a&1/2a	62.8	14.6	28.2	11.9	0.25	0.25	0.20	0.20
1/2m&1/4a	*	38.9	*	25.5	0.41	0.41	0.18	0.18
1/4m&1/2m&1/4a	*	29.8	*	22.2	0.23	0.23	0.13	0.13
1/4a&1/2a&1/2m	53.2	16.6	24.9	10.2	0.14	0.14	0.22	0.22

Notes: * indicates the error exceeds 100%, the underlined values are for regularization solution, and others for SVD solution.

Table 4 Comparison on RQPE of two axle time-varying loads Identified via SVD

Sensor location	1% Noise		5% Noise		10% Noise	
	Axle 1	Axle 2	Axle 1	Axle 2	Axle 1	Axle 2
1/4m&1/2m&3/4m	97.8	55.4	*	*	*	*
	7.35	1.81	36.7	9.03	73.5	18.1
1/4m&1/2m&1/2a	*	29.6	*	*	*	*
	4.45	1.50	22.3	7.50	44.5	15.0
1/4m&1/4a&1/2a	31.5	22.1	*	*	*	*
	1.31	0.76	6.54	3.81	13.1	7.62
1/4a&1/2a&3/4a	0.93	0.63	4.66	3.13	9.30	6.25
	0.86	0.31	4.29	1.56	8.58	3.11

Notes: * indicates the RQPE values exceeds 100%, the underlined values are for MOMA, and others for TDM.

when the SVD solution is adopted only. In addition, the effect of different noise levels on the RQPE values are also considered in Table 4. From Tables 3 and 4, some conclusions can be made as follows.

(1) For any of cases in both Tables 3 and 4, the MOMA results are obviously better than the TDM results whether for two constant load identification or for two time-varying load identification. For the cases of two axle constant load identification, the RQPE values by the MOMA are very low and less than 1.06% for all twelve cases in Table 3. They are dramatically lower than the RQPE values by the TDM. It shows that the MOMA is a very good identification method, which is especially suitable for two axle constant load identification.

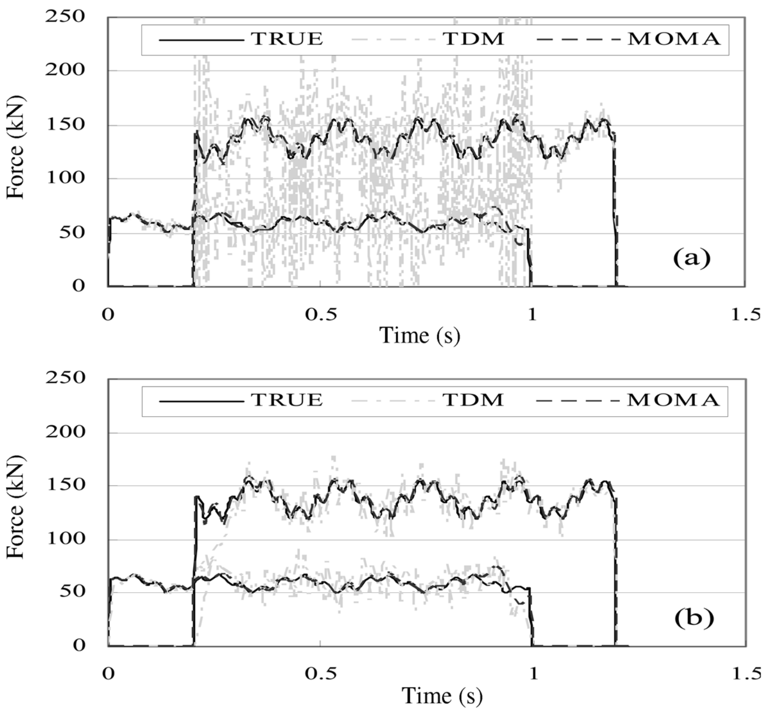

Fig. 6 Two axle time-varying load (1/4m&1/2m&3/4m 1% Noise) (a) With SVD Solution (b) With Regularization Solution

(2) Compared the SVD results with the regularization results, it can be found from Table 3 that the RQPE values for all cases, except for the case of 1/4a&1/2a&3/4a, are significantly reduced if the regularization solution are adopted instead of the SVD solution for the TDM. For the MOMA, the RQPE values are also significantly improved when the bending moment responses are only used to identify the two moving loads. However, when only the acceleration responses, or the combination of acceleration and bending moment responses are used to identify the two moving loads, the RQPE values are close to each other whether the SVD or the regularization solution is adopted.

(3) For case comparison, Table 3 also shows that, the more the measurement station is, or the more the number of measured acceleration involved is, the better the identified results are. It shows that adopting more responses for two moving load identification is beneficial to both the TDM and the MOMA. From Table 4, it can be seen that the more the number of bending moment responses replaced with acceleration responses is, the better both the TDM and the MOMA results are. The best sensor arrangement is when all three sensors are accelerometers, i.e. 1/4a&1/2a&3/4a, for both the two methods.

(4) Fig. 6 shows the TDM and MOMA identified results from three bending moment responses at locations of 1/4m&1/2m&3/4m under 1% noise when the SVD (Fig. 6(a)) and regularization (Fig. 6(b)) methods are adopted respectively. It can be seen from Fig. 6 that the MOMA results are clearly better than that of TDM whether using the SVD or regularization methods, which means that the MOMA can overcome the solution of ill-posed problem to some extent. In addition, the TDM identification accuracy has been greatly enhanced if the regularization method is adopted

instead of the SVD method.

(5) It can also be found from Table 4 that the RQPE values are almost proportional to the noise levels. Obviously, the MOMA identification accuracy is higher than the TDM accuracy for each case. It shows that the MOMA immunity to the noise is higher than the TDM immunity when 1%, 5% and 10% noise were added into the responses. In other words, the proposed MOMA method is more suitable for identification of moving loads from the measured response signals contaminated by measurement noise.

3.2.3 Multi-axle vehicle loads

Bending moment and/or acceleration responses at 1/5, 2/5, 3/5 and 4/5 spans in 10 combinations described in Table 5 are used to identify the three axle loads. In a manner similar to single and two axle load identification, the following conclusions are obtained.

(1) When no noises are added into the responses, the accurate results are obtained. This means that the MOMA and TDM are correct and are suitable for the identification of both three axle constant and time-varying loads.

(2) For the three axle constant load identification, when the regularization method is adopted and 1% noises are added into the responses, the QRPE values from both the TDM and MOMA are shown in Table 5. It can be found from Table 5 that the MOMA has higher accuracy and it can provide better results than the TDM although the TDM results have been greatly improved if they are compared with the SVD results.

(3) For the time-varying load identification, when 1% noises are added into the responses, the QRPE values from both the TDM and MOMA are shown in Table 6 when the regularization is adopted. It can be found that although the MOMA identification results are better than the TDM results, both of them have higher QRPE values. Compared with the RQPE values by the SVD, it can be seen that the two methods have been greatly improved and become effective if the regularization method is adopted, but the corresponding QRPE values are still higher than the expected. As a reference, Fig. 7 also plots the best identified results of the two methods. It can be seen that the MOMA results are better than the TDM.

Table 5 Comparison on RQPE of three axle constant loads identified via regularization

Sensor location	1% Noise					
	TDM			MOMA		
	Axle 1	Axle 2	Axle 3	Axle 1	Axle 2	Axle 3
1/5m&2/5m&3/5m&4/5m	46.9	21.1	23.2	0.29	0.21	0.18
1/5a&2/5a&3/5a&4/5a	14.5	16.0	18.8	0.15	0.09	0.05
1/5a&2/5a&3/5a&1/5m	19.9	17.2	19.5	0.50	0.00	0.07
1/5a&2/5a&3/5a&2/5m	18.7	17.1	19.6	0.06	0.18	0.01
2/5a&3/5a&1/5m&2/5m	21.2	17.8	19.5	0.26	0.02	0.07
2/5a&3/5a&2/5m&3/5m	22.0	17.5	20.1	0.11	0.11	0.03
1/5a&1/5m&2/5m&3/5m	39.4	19.5	21.4	0.31	0.15	0.09
2/5a&1/5m&2/5m&3/5m	41.9	20.1	21.6	0.07	0.08	0.05
1/5a&2/5a&3/5a&2/5m&3/5m	18.1	16.8	19.5	0.12	0.17	0.01
2/5a&3/5a&1/5m&2/5m&3/5m	21.5	17.3	19.3	0.27	0.03	0.02

Notes: 1/5, 2/5, 3/5 and 4/5 represent the measurement location at 1/5, 2/5, 3/5 and 4/5 span respectively.

Table 6 Comparison on RQPE of three axle time-varying loads Identified via regularization

Sensor location	1% Noise					
	TDM			MOMA		
	Axle 1	Axle 2	Axle 3	Axle 1	Axle 2	Axle 3
1/5m&2/5m&3/5m&4/5m	47.2	20.8	25.2	29.4	13.6	17.8
1/5a&2/5a&3/5a&4/5a	17.4	16.7	21.2	17.4	13.4	17.1
1/5a&2/5a&3/5a&1/5m	21.9	17.5	21.6	18.9	13.4	16.3
1/5a&2/5a&3/5a&2/5m	20.5	17.6	21.8	17.4	13.5	16.2
2/5a&3/5a&1/5m&2/5m	21.7	17.5	21.0	18.0	13.9	17.0
2/5a&3/5a&2/5m&3/5m	22.2	17.2	21.5	17.8	13.9	17.6
1/5a&1/5m&2/5m&3/5m	39.7	19.2	23.6	28.7	14.9	18.6
2/5a&1/5m&2/5m&3/5m	42.3	19.9	23.7	25.9	14.1	17.2
1/5a&2/5a&3/5a&2/5m&3/5m	19.9	17.2	21.5	17.1	13.1	15.9
2/5a&3/5a&1/5m&2/5m&3/5m	21.7	17.0	20.9	17.2	13.8	17.0

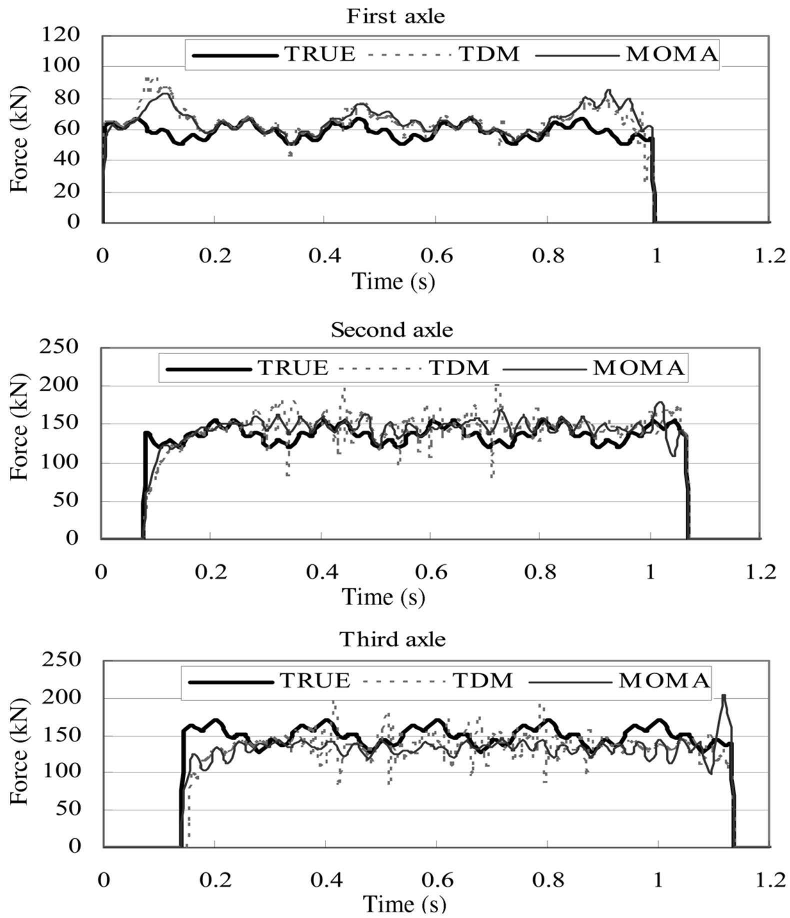

Fig. 7 Identified Three axle Time-varying loads with regularization (1/5a&2/5a&3/5a&4/5a 1% Noise)

3.3 Accuracy and discussion

3.3.1 Evaluation on MOMA

(1) Simulation results above all show that the MOMA is better than the existing TDM from all the aspects. The MOMA has higher identification accuracy and robust immunity to noise. It is a very good identification method for moving loads on bridge, especially for the constant load identification.

(2) The basis function has a great effect on the MOMA. The different patterns of basis functions will cause different computation efficiency. In this paper, two basis functions are adopted for the MOMA and have been further studied. The results show that the Fourier basis function is better than the Legendre basis function because of its higher efficiency and accuracy. In order to increase the accuracy and to save the computational cost, further study is required to optimize the basis function so that the basis function features can be fully understood and made better use of.

(3) As the basis function was adopted finally, the basis function number should be determined with care. The different the basis function number is, the different the identification accuracy and efficiency is in practice. In general, the more the basis function number is, the higher the MOMA identification accuracy is, but it also causes higher computational cost and greater effect due to the ill-posed problem (Chew *et al.* 2001). Therefore, the basis function number should be appropriately determined in order to keep the MOMA more effective.

3.3.2 effect of vehicle axle

(1) With the vehicle axle increasing, the TDM identification accuracy has been reduced and its computational cost has been increased largely, whether for the constant load identification or for the time-varying load identification cases. The satisfactory results could be only obtained for the single force identification if the TDM is used to identify the moving vehicle loads.

(2) Vehicle axle has no effect on the MOMA in terms of computational cost and accuracy for the constant load identification. Although the accuracy for multiple axle time-varying load identification is reduced, the MOMA can still provide the better results and higher efficiency than the TDM.

3.3.3 Effect of noise

(1) The TDM is sensitive to the noise when the bending moment responses are only used to identify the constant or time-varying moving loads. If the bending moment responses are partly or completely replaced with the acceleration responses, the TDM results can be improved clearly.

(2) The MOMA are less sensitive to the noise when it is used to identify the constant moving loads for all cases. For the time-varying load identification cases, although the MOMA results are worse than those for the constant moving load cases, the MOMA accuracy is still higher than the TDM. Both the TDM and the MOMA identification results could be improved if the regularization method is adopted, especially for the TDM.

4. Conclusions

In this paper, a MOM-based algorithm (MOMA) has been proposed for the identification of moving loads on bridges. Based on the numerical simulation results, the following conclusions can be made. (1) The proposed MOMA is a successful method for the identification of moving loads from the responses induced by the moving vehicles on bridges. (2) The MOMA is obviously better than the existed TDM from all the aspects, especially for the constant load identification cases. (3) The MOMA can give satisfactory results with higher accuracy and efficiency when whether the SVD or regularization method is used. (4) The MOMA has robust immunity to the noise. It can improve the solutions of ill-posed problem to some extent. (6) It is recommended to use regularization method as the bending moment responses are only used to predict the time-varying loads, especially for the TDM.

In order to evaluate the proposed MOMA, further experiment evaluation and comparative studies have been done and will be provided in a separate report.

Acknowledgements

The project is jointly supported by the National Natural Science Foundation of China (50378009), the Key Project of Chinese Ministry of Education of China (208172), the Foundation of Talent Program of Jinan University (51207052), the funding of the Key Lab of Diagnosis of Fault in Engineering Structures, Guangdong Province of the People's Republic of China (Jinan University), and the Hong Kong Polytechnic University Postdoctoral Fellowship Research Grants (G-YX25). The support by the Queensland University of Technology is also gratefully acknowledged.

References

Busby, H.R. and Trujillo, D.M. (1997), "Optimal regularization of an inverse dynamic problem", *Comput. Struct.*, **63**(2), 243-248.

Cantineni, R. (1992), "Dynamic behaviour of highway bridges under the passage of heavy vehicles", Swiss Federal Laboratories for Materials Testing and Research (EMPA) Report No. 220, 240.

Chan, T.H.T. and O'Conner, C. (1990), "Wheel loads from highway bridge strains: Field studies", *J. Struct. Eng.*, ASCE, **116**(7), 1751-1771.

Chan, T.H.T., Yu, L. and Law, S.S. and Yung, T.H. (2001), "Moving Force Identification Studies II: Comparative Studies", *J. Sound Vib.*, **247**(1), 77-95.

Chan, T.H.T., Yu, L., Law, S.S. and Yung, T.H. (2001), "Moving Force Identification Studies I: Theory", *J. Sound Vib.*, **247**(1), 59-76.

Fast and efficient algorithms in computational electromagnetics. Chew W.C., Jin J.M. Michielssen E., Song J. Eds. Artech House. Norwood. MA, 2001.

Harriington, R.F. (1968), *Field Computation by Moment Methods*. New York: Macmillan.

Heywood, R.J. (1994), "Influence of truck suspensions on the dynamic response of a short span bridge", *Int. J. Vehicle Des*.

Jorgensen, E., Volakis, J.L., Meincke, P. and Breinbjerg, O. (2004), "Higher order hierarchical Legendre basis functions for electromagnetic modeling", *IEEE T. Antenn. Propag.*, **52**(11), 2985-2995.

Law, S.S., Chan, T.H.T. and Zeng, Q.H. (1997), "Moving force identification: A time domain method", *J. Sound Vib.*, **201**(1), 1-22.

Law, S.S., Chan, T.H.T., Zhu, X.Q. and Zeng, Q.H. (2001), "Regularization in moving force identification", *J. Eng. Mech.,* ASCE, **127**(2), 136-148.

Liao, S.X. and Pawlak, M. (1996), "On image analysis by moments", *IEEE T. Pattern Anal.*, **18**(3), 254-266.

Lindfield, G. and Penny, J. (1995), *Numerical Method using Matlab*. London: Ellis Horwood Limit.

Pawlak, M. (1992), "On the reconstruction aspects of moment descriptors", *IEEE T. Inform. Theory*, **38**(6), 1698-1708.

Peters, R.J. (1984), "A system to obtain vehicle axle weights", *Proc. of 12th ARRB Conf.*, **12**, 10-18.

Peters, R.J. (1986), “An unmanned and undetectable highway speed vehicle weighing system”, *Proc. of 13th ARRB and 5th REAAA Combined Conf. Part 6,* 70-83.

Poularikas, A.D. (1999), Legendre Polynomial. In. The Handbook of Formulas and Tables for Signal Processing. Ed. Alexander D. Poularikas. Boca Raton: CRC Press LLC.

Qjidaa, H. and Radouane, L. (1999), “Robust line fitting in a noisy image by the method of moments”, *IEEE T. Pattern Anal.*, **21**(11), 1216-1223.

Santantamarina, J.C. and Fratta, D. (1998), “Introduction to discrete signals and inverse problems in civil engineering”, ASCE, Reston. Va., 200-238.

Tikhonov, A.N. and Arsenin, V.Y. (1977), *Solution of Ill-posed Problems*. Wiley. New York.

Ting, E.C. and Yener, M. (1983), “Vehicle-structure interaction in bridge dynamic”, *Shock Vib. Dig*., **15**(2), 3-9.

Yu, L. (2002), “Accounting for bridge dynamic loads using moving force identification system (MFIS)”, Hong Kong: The Hong Kong Polytechnic University.